ISSN 0036-0295, Russian Metallurgy (Metally), Vol. 2014, No. 10, pp. 800–806. © Pleiades Publishing, Ltd., 2014.
Original Russian Text © S.A. Lur'e, P.A. Belov, 2013, published in Deformatsiya i Razrushenie Materialov, 2013, No. 5, pp. 10–17.

DEFORMATION AND FRACTURE MECHANICS

Scale Effects in Brittle Fracture Mechanics

S. A. Lur'e[a, *] and P. A. Belov[b]

[a] *Institute of Applied Mechanics, Russian Academy of Sciences, Leninskii pr. 32a, Moscow, 119991 Russia*
**e-mail: lurie@ccas.ru*

[b] *Bauman State Technical University, ul. Vtoraya Baumanskaya 5, Moscow, 105005 Russia*

Received January 9, 2013

Abstract—The test problem of brittle fracture mechanics for a mode I crack is considered, and the asymptotics of solution is constructed in the vicinity of a crack tip using a gradient theory of deformation, which takes into account scale effects. It is shown that, in contrast to the classical theory of elasticity, the gradient theory can be used to obtain nonsingular solutions at the crack tip at various degrees of accuracy, which makes it possible to refine the trajectories of the limiting stresses and to substantiate the classification of brittle fracture mechanisms depending on the scale structural parameters (characteristic grain size).

DOI: 10.1134/S0036029514100061

1. INTRODUCTION

To describe the deformation and fracture of new materials with a micro- and nanostructure adequately, it is necessary to develop models for deformed media that take into account the structure of such materials. This explains the development of deformation models that go beyond the scope of the classical theory of elasticity. Gradient theories of elasticity and plasticity, which can comprehensively describe local short-range interactions, are promising in this field.

The first versions of gradient deformation models were likely to be developed in the early 1980s. In the 1990s, they were improved as gradient theories of elasticity and plasticity [1–4]. These investigations then served as a theoretical basis for applied gradient theories that take into account dislocation fields and damages during deformation, the interfacial properties near interfaces in heterogeneous materials, and the scale effects in the problems of the mechanics of composite materials [5–7].

The authors of [7–9] showed that gradient theories can be effectively used to describe the properties of microstructures and the deformation of miniature device components. In recent works [10–14], first-order gradient theories were developed using consistent variational models for media with conserved dislocations. These models are intended for predicting the scale effects in the volume and the surface adhesion properties of deformed media. The authors of [15–18] proposed an applied model for an interface layer; this model contains the minimum number of parameters for simulating the adhesion interactions between various components (adhesion damage at contact boundaries) and only one additional physical parameter to take into account the scale effect of a cohesion field.

In this work, the interface layer model is used to construct an asymptotic solution to a model problem of fracture mechanics.

2. FORMULATION OF THE GRADIENT DEFORMATION THEORY

We now consider the applied linear theory of interface layer that is a particular case of the gradient deformation theories [13–17]. The mathematical formulation of the edge problem of the interface layer theory follows directly from the following variational model:

$$\delta L = \delta(A - E) = 0,$$
$$E = \int_G E_G dV + \int_{\partial G} E_{\partial G} dV', \qquad (1)$$
$$A = \int_G A_G dV + \int_{\partial G} A_{\partial G} dV'.$$

Here, A is the work of given external forces distributed over volume V and surface V' of the elastic body; E is the potential energy of deformation; and E_G and $E_{\partial G}$ are the potential energy densities of deformation in the volume and on the surface, respectively. In this case, we have

$$E_G = (1/2)(2\mu\varepsilon_{ij}\varepsilon_{ij} + \lambda\theta^2 + Cu_iu_i),$$
$$E_{\partial G} = D_{ij}\dot{R}_i\dot{R}_j/2. \qquad (2)$$

Here, $\varepsilon_{ij} = (R_{i,j} + R_{j,i})/2$ is the strain tensor, where $R_{i,j} = \partial R_i/\partial x_j$ and R_i is the displacement vector; $\theta = R_{i,k}\delta_{ik} = \operatorname{div} R$ is the spherical part of the strain tensor; $D_{ij} = An_in_j + B(\delta_{ij} - n_in_j)$ is the characteristic of the adhesion stresses, where A and B are the physical con-

stants that determine the "normal" and "shear" adhesion; $\dot{R}_i = (\partial R_i/\partial x_j)n_j$ is the normal derivative of the displacement vector, where n_i is the vector of normal to the surface; and C is the additional physical constant that takes into account scale effects and determines the contribution of local cohesion-type gradient interactions to strain energy density E_G in the body volume.

The gradient components in Eq. (2) are determined by cohesion displacement vector u_i [13, 15–17]; in the interface layer model (Eqs. (1), (2)), it is determined by the equality

$$u_i = (-(1/C))L_{ij}(R_j).$$

where $L_{ij}(...) = \mu(...)_{,pp}\delta_{ij} + (\mu + l)(...)_{,ij}$ is the classical Lamé operator, δ_{ij} is the Kronecker delta, and μ and λ are the Lamé coefficients.

Gradient component Cu_iu_i determines the strain energy versus the strain curvature. This follows from the definition of gradient displacement field u_i if we take into account that

$$L_{ij}(R_j) = C_{ijmk}R_{m,kj},$$

where $C_{ijnm} = \lambda\delta_{ij}\delta_{nm} + \mu(\delta_{in}\delta_{jm} + \delta_{im}\delta_{jm})$ is the elastic modulus tensor.

It should be noted that, in the model proposed in [3], the cohesion displacement field is determined in terms of the Laplace operator rather than the Lamé operator. This "simplification" is related to the assumption of the equality of the scale parameters that determine the lengths of the shear- and dilation-induced local gradient effects.

Variational equations (1) and (2) give the following set of equations for total displacement vector R_k for the model under study (Euler equations):

$$\begin{gathered} L_{ij}H_{jk}(R_k) + P_i^G = 0, \\ L_{ij}(...) = \mu(...)_{,pp}\delta_{ij} + (\mu + \lambda)(...)_{,ij}, \\ H_{jk} = (...)\delta_{jk} - L_{jk}(...)/C, \end{gathered} \tag{3}$$

where P_i^G is the vector of forces distributed in the volume.

The general solution to Eq. (3) for full displacement vector R_k can be represented as the sum of the vectors of "classical" (U_i) and "cohesion" (u_i) displacements [14, 16],

$$R_i = U_i - u_i, \quad -CH_{ij}(u_j) + P_i^G = 0, \tag{4}$$

where $u_i = -(1/C)L_{ij}(R_j)$ and $U_i = H_{ij}(R_j)$.

Cohesoin field vector u_i can be represented in the form $u_i = -(1/C)C_{ijmk}R_{m,kj}$, which can be easily shown if the equality $L_{ij}(R_j) = C_{ijmk}R_{m,kj}$ is taken into account. Then, with allowance for equality (4), the expression for the strain energy density in Eq. (2) can be rewritten as

$$E_G = (1/2)(C_{ijnm}R_{i,j}R_{n,m} + C_{ijknml}R_{i,jk}R_{n,ml}). \tag{5}$$

For the model under study, the tensor of the elastic moduli of gradient interactions in the expression for the strain energy density (Eq. (5)) has the simple form

$$C_{ijknml} = C_{ijrk}C_{nmrl}/C.$$

The stresses in the gradient theory can be found by Green's formula. From Eq. (2), we obtain

$$\sigma_{ij} = C_{ijnm}R_{n,m}.$$

With allowance for decomposition (4), stress tensor σ_{ij} can be written as the decomposition

$$\sigma_{ij} = s_{ij} + t_{ij},$$

where $s_{ij} = C_{ijnm}U_{n,m}$ are the classical stresses and $t_{ij} = C_{ijnm}u_{n,m}$ are the cohesion stresses. Cohesion stresses t_{ij} satisfy the equilibrium equations $t_{ij,j} - Cu_i + P_i^G = 0$ [14].

The variational equation that corresponds to the requirement of stationary Lagrangian in Eq. (1) has the form (with allowance for Eqs. (2) and (5))

$$\begin{aligned} \delta L = &\int_G [C_{ijrk}(R_r - C_{nmrl}R_{n,lm}/C)_{,jk} + P_i^G]\delta R_i dV \\ &+ \int_{\partial G} [P_i^{\partial G} - C_{ijrk}n_j(R_r - C_{nmrl}R_{n,lm}/C)_{,k}]\delta R_i dV' \\ &- \int_{\partial G} (C_{rqnm}R_{n,qm}/C)\delta(C_{rpij}n_pR_{i,j})dV' = 0, \end{aligned} \tag{6}$$

where n_j is the unit vector normal to the body surface ∂G and P_i^G and $P_i^{\partial G}$ are the vectors of the given forces distributed over the volume and surface of the body, respectively.

The vectors of the classical and cohesion displacement components are determined in terms of total displacement vector $R_i (R_i = U_i - u_i)$ using the formulas

$$\begin{gathered} U_i = R_i - C_{ijnm}R_{n,jm}/C, \\ u_i = -C_{ijnm}R_{n,m}/C. \end{gathered}$$

3. FORMULATION OF THE PROBLEM OF FRACTURE MECHANICS

We now consider the simplified problem of fracture mechanics for a mode I crack in the case of plane strain state. The elastic body with a crack to be studied is assumed to be incompressible along the longitudinal coordinate. A semi-infinite crack propagates along the longitudinal coordinate axis ($x \geq 0$, $y = 0$). In this case, the displacement field is determined by only one displacement vector component $R(x, y) = U - u$ along axis OY,

$$R_iY_i = R(x, y), \quad R_iX_i \equiv 0,$$

where $\{X_i\}$ and $\{Y_i\}$ are the coordinate axis vectors in the independent orthogonal coordinate system.

We also assume that mass and surface forces are absent. Therefore, the work of external forces in Eq. (1) is taken to be $A = 0$. The surface properties of the crack edges are not taken into account, i.e., $D_{ij} = 0$ and, hence, $E_{\partial G} = 0$ (see Eq. (2)).

For the model problem under study the expression that determines the strain energy density in the volume in Eq. (2) taks the simple form

$$E_G = (1/2)[\mu R_{,x}R_{,x} + (2\mu + \lambda)R_{,y}R_{,y} + Cuu].$$

Then, we take into account Eq. (5) and easily find that the fundamental solution corresponding to total displacement vector $R(x, y)$ satisfies the equilibrium equation (Euler equation in Eq. (6))

$$\nabla^2[l_E^2\nabla^2 R - R] = 0. \quad (7)$$

Here, $\nabla^2(\ldots) = \partial^2(\ldots)/\partial\bar{x}^2 + \partial^2(\ldots)/\partial y^2$ is the plane Laplace operator in "extended" coordinates, where $\bar{x} = x\sqrt{(2\mu + \lambda)/\mu}$ is extended coordinate x and $l_E = \sqrt{(2\mu + \lambda)/C}$ is the scale parameter.

Recall that the only displacement R component in the particular case under study is represented as decomposition into classical and cohesion displacement components; that is, $R = U - u$,

$$U = R - l_E^2\nabla^2 R, \quad u = -l_E^2\nabla^2 R. \quad (8)$$

The fundamental solution that corresponds to the classical displacement component satisfies the equation

$$\nabla^2 U = 0. \quad (9)$$

Here, $U = U_iY_i = U(\bar{x}, y)$ is the desired component of the classical displacement vector and Y_i is the unit vector of axis OY.

The fundamental solution for the cohesion displacement has the form

$$l_E^2\nabla^2 u - u = 0, \quad (10)$$

where $u = u_iY_i = u(\bar{x}, y)$ is the desired component of the cohesion displacement vector.

The fundamental solutions to Eqs. (7), (9), and (10) are constructed in the polar coordinate system $\{r, \varphi\}$, where r is the radius vector of the point under study and φ is the angle measured counterclockwise from the upper crack edge.

For the model problem under study, the normal stresses along axis OX are zero. Normal stresses $\sigma_y \equiv \sigma$ alog axis OY and shear stresses τ are written with Green's formulas as

$$\sigma = (2\mu + \lambda)R_{,y} = (2\mu + \lambda)[U_{,y} - u_{,y}],$$

$$\tau = \mu R_{,x} = \mu[U_{,x} - u_{,x}].$$

4. CLASSICAL SOLUTION FOR A MODE I CRACK

To achieve the classical solution, we assume that $l_E = 0$ and, correspondingly, $C^{-1} = 0$. Then, for the model problem of a mode I crack, it directly follows from variational equation (6) that the classical stresses ($s = \sigma$, $U = R$) should be zero, i.e., $\sigma = (2\mu + \lambda)R_{,y}$ at the crack edges ($x \geq 0$, $y = 0$). We can easily show that the following asymptotic solution takes place in this case in the vicinity of the crack tip:

$$R(r, \varphi) = 2K_Ir^{1/2}\cos(\varphi/2)/(2\mu + \lambda),$$
$$\sigma = K_Ir^{-1/2}\sin(\varphi/2), \quad (11)$$

where K_I is the stress intensity factor.

We now search for the trajectories of the critical stresses, i.e., the stresses for which the operating stresses become equal to the ultimate tensile strength or the yield strength ($\sigma = \sigma_c$). Let $\sigma = \sigma_c$ and $K_I = K_{Ic}$, where K_{Ic} is the critical stress intensity factor (fracture toughness), in Eq. (11). Then, from Eq. (11), we obtain the following equation for the critical stress trajectory:

$$z(\varphi) = q^2\sin^2(\varphi/2), \quad (12)$$

where $q = K_{Ic}/\sigma_c l_E^{1/2}$ and $z = r/l_E^{1/2}$.

We now determine the characteristic size d of the region that can be exfoliated when the critical stresses are reached. To this end, we average the dependence $r = r(\varphi)$ over the angle. From Eq. (12), we obtain

$$d = (1/\pi)\int_0^{2\pi} r(\varphi)d\varphi = (K_{Ic}/\sigma_c)^2. \quad (13)$$

It is important that the following relation between the yield stress and the characteristic region size, which is analogous to the Hall–Petch relation, follows from Eq. (13):

$$\sigma_c = K_{Ic}d^{-1/2}.$$

We take into account Eq. (13) and rewrite the expression for the stress in Eq. (11) in the form

$$\sigma = \sigma_c(K_I/K_{Ic})(r/d)^{-1/2}\sin(\varphi/2). \quad (14)$$

It can easily be seen from Eq. (14) that the stresses inside the region $r < d$ become higher than the critical stresses and that they are infinite in the vicinity of the crack tip ($r \to 0$). Thus, the classical theory can predict the mechanism of brittle fracture characterized by the separation of the fragment that is symmetrically located in front of the crack tip and has characteristic size d_c.

The stresses in Eq. (14) reach the yield strength in the trajectory of a fragment of critical size $d = d_c$. The equations of the theory of elasticity are considered to be valid outside the fragment, at a certain distance

from its contour. If the fragment has the sizes sufficient for it can be taken as "representative volume," the scenario of its fracture should not differ from scenario of the entire medium. If the medium has an internal (e.g., polycrystalline) structure and the fragment size is sufficiently close to the crystallite size, the scenario of fracture should change substantially. At $d < d_c$, the nonclassical effects that cannot be explained in terms of the classical theory of elasticity would be observed. One of these characteristic effects is a systematic deviation from the Hall–Petch relation, which is detected for materials having a micro- or nanostructure, i.e., materials with a very small grain size. Such nonclassical scale effects are assumed to be simulated using the gradient theory of elasticity.

5. GRADIENT SOLUTION

Let us consider gradient model (1) and construct asymptotic nonsingular solutions for stresses. It can easily be checked that the asymptotics of total stresses $\sigma = s + t$ for the model problem of a mode I crack allows a simulation in the form of a linear combination of the asymptotics of classical (s) and cohesion (t) stresses [14],

$$\begin{aligned} s &= K_I l_E^{1/2} z^{-1/2} \sin(\varphi/2), \\ t &= -(2/\pi)^{1/2} (K_I l_E^{1/2} K_{1/2}(z)) \sin(\varphi/2), \end{aligned} \tag{15}$$

where $K_{1/2}(z)$ is the cylindrical half-integer-order Macdonald function and $z = r/l_E$.

We take into account the asymptotic properties of Macdonald function $K_{1/2}(z)$ at $|z| \to 0$. We can easily find with Eq. (15) that the total stress written as the sum $\sigma = s + t$ describes the nonsingular solution at the crack tip $|z| \to 0$ that has the asymptotics of classical solution (11) at infinity ($r \to \infty$),

$$\sigma = K_I l_E^{1/2} (1 - e^{-z}) z^{-1/2} \sin(\varphi/2). \tag{16}$$

Note that the corresponding displacements of the crack edges can be obtained by integrating Eq. (16) with allowance for the fact that $\partial/\partial y = \partial/(R\partial\varphi)$ at the crack edges. In [15], we showed that the expressions thus derived describe the opening of the edges of a mode I crack that corresponds to so-called equilibrium cracks. In this case, the angle between the crack edges at the crack tip is zero.

We consider the equation of critical trajectories for the obtained gradient solution. Assuming $K_I = K_{Ic}$ and $\sigma = \sigma_c$ in Eq. (16), we have

$$z^{1/2}/(1 - e^{-z}) = q \sin(\varphi/2), \tag{17}$$

where $q = K_{Ic}/l_E^{1/2} \sigma_c$.

Note the following. An analysis of Eq. (17) shows that there is the sufficiently low value of parameter q such that this equation has no roots for $\varphi = \pi$. Therefore, there is the characteristic size of a material structure such that the scenario of fracture related to the exfoliation of the material fragment symmetrically located in front of the crack tip. In this case, fracture is likely to be associated with the exfoliation of two or more fragments. To refine the scenario of possible fracture and to reveal its dependence on the scale factor, we consider the refined asymptotics of the solution in the vicinity of the crack tip.

6. REFINED GRADIENT SOLUTION

Note that asymptotic regular solution (16) for stresses was obtained from the assumption that the singularity of the classical solution is compensated for by the singularity of the cohesion solution. However, this solution is not unique and complete. We will find a more complete asymptotic solution, which will refine the stress distribution. To this end, we again consider the problem of a mode I crack and write the solution to Eq. (7) in the form

$$\begin{aligned} R(z, \varphi) &= l_E \left\{ A_1 z^{-1/2} - C_1 K_{1/2}(z) + \frac{2K_I}{(2\mu + \lambda) l_E^{1/2}} z^{1/2} \right\} \\ &\times \cos(\varphi/2), \end{aligned} \tag{18}$$

where A_1 and C_1 are constants to be determined below.

The total stresses are

$$\begin{aligned} \sigma(z, \varphi) &= \left\{ [-A_1 z^{-3/2} + C_1 K_{3/2}(z)] \sin(3\varphi/2) \right. \\ &\left. + \left[\frac{2K_I}{(2\mu + \lambda) l_E^{1/2}} z^{-1/2} + C_1 K_{1/2}(z) \right] \sin(\varphi/2) \right\} \\ &\times (2\mu + \lambda)/2, \end{aligned} \tag{19}$$

where $K_{1/2}(z)$ and $K_{3/2}(z)$ are the half-integer-order Macdonald functions.

Obviously, the requirement of the nonsingularity of total displacements (18) is met under the condition $A_1 = C_1 \sqrt{\pi/2}$. In this case, we can check that the nonsingularity of total stresses (19) also takes place despite the fact that to singularities appear in the stresses in the general case. The first singularity is on the order of $z^{-1/2}$ and the second is one the order of $z^{-3/2}$. Nevertheless, eliminating the classical singularity using the equality $C_1 \sqrt{\pi/2} = -2K_I l_E^{1/2}/(2\mu + \lambda)$, we can find that the nonclassical singularity loses two orders of magnitude due to the fact that the requirement of regularity of total displacements was preliminarily met. Here, we used the property of half-integer-order Macdonald functions that allows on to express them in terms of elementary functions.

As a result, the expressions for total displacements and total stresses become nonsingular. Finally, the

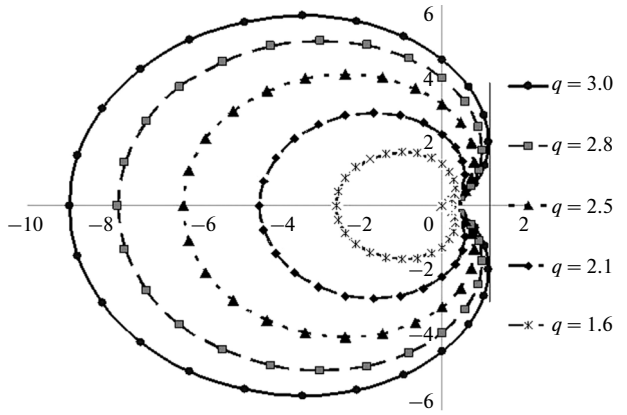

Fig. 1. Trajectories of the critical stresses for classical solution (12).

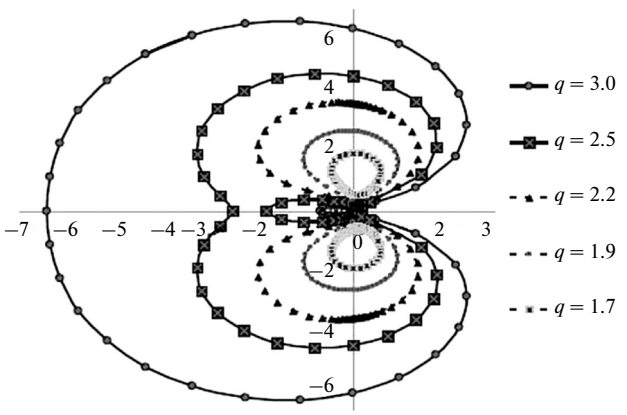

Fig. 2. Trajectories of the critical stresses for gradient solution (22).

expressions for the displacements are reduced to the form

$$R(z, \varphi) = [2K_{\mathrm{I}} z^{-1/2} l_E^{1/2}/(2\mu + \lambda)](e^{-z} - 1 + z)\cos(\varphi/2). \quad (20)$$

The total stresses are written as

$$\sigma(z, \varphi) = K_{\mathrm{I}} l_E^{-1/2} z^{-3/2}(1 - e^{-z} - ze^{-z}) \times \sin(3\varphi/2) + (1 - e^{-z}) z^{-1} \sin(\varphi/2). \quad (21)$$

This solution takes into account higher variability of the solution in the angular coordinate. Note that this process of refining can be continued.

7. ANALYSIS OF THE SOLUTION

Equation (20) describes the profile of crack edges and shows that the nonclassical solution gives a zero opening angle between the crack edges at the tip. It is well known that the opening angle at the tip for the classical solution is π. Obviously, the function that determines the displacement of the crack edges in Eq. (20) has an inflection point. The coordinate of the inflection point almost coincides with scale parameter l_E. Therefore, we can treat this parameter as a material characteristic in the mechanics of brittle fracture.

Using solution (21), we write equations for critical stress trajectories. For this purpose, we assume $K_{\mathrm{I}} = K_{\mathrm{Ic}}$ and $\sigma = \sigma_c$ and introduce critical parameter $q = K_{\mathrm{Ic}}/\sigma_c l_E^{1/2}$. Then, an equation for the critical stresses can be written as

$$f(z, \varphi, q) = 0, \quad (22)$$

where

$$f(z, \varphi, q) = qz^{-1/2}\{[(1 - e^{-z}) - ze^{-z}] \times \sin(3\varphi/2) + (1 + e^{-z})\sin(\varphi/2)\} - 1.$$

Figures 1 and 2 show the trajectories of the limiting stresses for the classical and gradient solutions. These trajectories are plotted using Eqs. (12) and (22) for various values of critical parameter q. For each fixed value of parameter q, z is explicitly found by solving the corresponding transcendental equation. Such solutions were obtained for fixed values of angle φ_i. In the calculations, we used an angular step of π/18 and derived dependences $z = z(\varphi, q)$.

The limiting stress trajectories determine the regions in the vicinity of the crack tip at the boundaries of which the stresses reach critical values. Inside these regions, the stresses exceed the critical values.

For low values of z, the critical stress trajectories plotted according to the classical and gradient solutions differ substantially. For high values of z, the inequality $e^{-z} \ll 1$ holds true. Therefore, the equation of the critical stress trajectory in the gradient solution is simplified in this case and can be explicitly written as

$$z = (K_{\mathrm{Ic}}/\sigma_c l_E^{1/2})^2 \sin^2(\varphi/2).$$

It can easily be seen that it coincides with Eq. (12), which was derived using the classical solution (also see Eq. (17)). Thus, the solutions found using the classical theory of elasticity and the gradient model agree with each other accurate to $O(z^{-1})$ outside the region with the characteristic size $d_c = (K_{\mathrm{Ic}}/\sigma_c)^2$. Correspondingly, for higher values of z, the critical stress trajectories for the classical and gradient solutions are close to each other.

When analyzing the obtained dependences, we find the threshold value of parameter $q = q_c$ at which one rather than two roots exists for the case $\varphi = \pi$. We found that $q_c = 2.489$ and a single root ($z_c = 2.149$) exists in this case.

Note that the fracture mechanism changes qualitatively at $q_c = 2.489$: two fragments instead of one fragment are exfoliated from the medium symmetrically relative to the crack plane (see Fig. 2).

At $q > q_c$, we have a classical solution and the critical stress trajectory is closed. In this case, Eq. (22) has two roots at $\varphi = \pi$.

At $q = q_c$, the trajectory is self-intersecting and Eq. (20) has one root at $\varphi = \pi$.

At $q < q_c$, two closed trajectories that are symmetric relative to axis OX appear in the upper and lower half-planes. In this case, Eq. (22) has no roots at $\varphi = \pi$.

We now repeat the procedure of constructing the analog of the Hall–Petch relation. To this end, we average the $z = z(\varphi, q)$ dependence over the angle. As a result, similarly to Eq. (11), we can find the relation between characteristic size d and parameter q,

$$d = 2l_E\frac{1}{\pi}\int_0^\pi z(\varphi, q)d\varphi = d(q).$$

From this equation, we can find the pairs of d and q that determine parametric dependence $d = d(q)$. The inversion of this dependence leads to the classical formulation of the relation, which can be called the generalization of the Hall–Petch relation,

$$\sigma_c = \frac{K_{1c}}{q(d/l_E)l_E^{1/2}}. \quad (23)$$

As follows from a comparison of Eq. (23) with the expression $\sigma_c = K_{1c}d^{-1/2}$ (see Eq. (13)), parameter q at highvalues of d/l_E has the asymptotics $\lim_{(d/l_E)\to\infty} q(d/l_E) = (d/l_E)^{1/2}$. Therefore, the classical Hall–Petch relation does hold true at relatively high values of d/l_E. However, it is clearly seen that Eq. (23) gives another forecast at low values of parameter d/l_E, i.e., at a small characteristic size in a material structure: a decrease in the characteristic structure element size results in a decrease in the limiting stresses (yield strength) as compared to the classical Hall–Petch relation.

8. CONCLUSIONS

An analysis of the scenarios of brittle fracture that was performed with allowance for scale effects fully supports the validity of the classification of nanostructured media proposed in [19]. According to this classification, the size series of nanocrystals is divided into three groups, namely, large, medium, and small nanocrystals, where different fracture mechanisms dominate. These mechanisms are determined by a predominant structural element, i.e., crystals, grain boundaries, or triple junctions, respectively.

For example, at $d \geq d_c$ and $d_c = (K_{1c}/\sigma_c)^2$, the fracture mechanism is predicted in terms of a classical solution and related to the exfoliation of a representative fragment in front of the crack tip. The dependence of the yield strength on the characteristic structure element size is described by the Hall–Petch relation.

At characteristic structure element sizes $l_E < d < d_c$, the properties of the structure are determined by a refined gradient model. In this case, the scenario of brittle fracture is different: it is associated with fracture along the boundary of two fragments, which is accompanied by the exfoliation of two regions. This situation is characterized by a generalized nonclassical Hall–Petch relation, which predicts a decrease of the yield strength with decreasing characteristic structure parameter as compared to the classical Hall–Petch relation.

The case $d < l_E$ is also of particular interest; it is most likely to belong to nanocrystalline materials. This case should be considered with allowance for high-order refinements, which can be obtained in terms of a gradient theory. It can be shown that the trajectories of the limiting stresses in this case point to the exfoliation of three fragments.

ACKNOWLEDGMENTS

This work was supported by the Russian Foundation for Basic Research (project nos. 12-01-00273, 11-01,12081, 10-07-00040) and the federal program (project nos. 14.740.11.0995, 8221).

REFERENCES

1. E. C. Aifantis, "On the microstructural origin of certain inelastic models," J. Engng. Mater. Technol. **106**, 326–330 (1984).
2. E. C. Aifantis, "The physics of plastic deformation," Int. J. Plastisity **3**, 211–247 (1987).
3. B. S. Altan and E. C. Aifantis, "On some aspects in the special theory of gradient elasticity," J. Mech. Behav. Mater. **8** (3), 231–282 (1997).
4. E. C. Aifantis, "Gradient effects at the macro, micro and nano scales," J. Mech. Behav. Mater. **5**, 335–353 (1994).
5. E. C. Aifantis, "Strain gradient interpretation of size effects," Int. J. Fract. **95**, 299–314 (1995).
6. N. A. Fleck and J. W. Hutchinson, "A reformulation of strain gradient plasticity," J. Mech. Phys. **9**, 2245–2271 (2001).
7. K. E. Aifantis and J. R. Willis, "The role of interfaces in enhancing the yield strength of composites and polycrystals," J. Mech. Phys. Solids **53**, 1047–1070 (2005).
8. R. D. Mindlin, "Elasticity, piezoelectricity and crystal lattice dynamics," J. Elasticity **2** (4), 217–280 (1972).
9. G. A. Maugin, "Material forces: concepts and applications," Appl. Mech. Rev. **48**, 213–224 (1995).
10. S. Lurie and A. Kalamkarov, "General theory of continuous media with conserved dislocations," Int. J. Solids Struct. **44**, 7468–7485 (2007).
11. P. A. Belov and S. A. Lurie, "A continuum model of microheterogeneous media," Appl. Math. Mech. **73** (5), 833–848 (2009).
12. S. A. Lurie, P. A. Belov, and N. P. Tuchkova, "Gradient theory of media with conserved dislocations: application to microstructured materials," in *One Hundred*

Years after the Cosserats. Series: Advances in Mechanics and Mathematics (Springer, New York, 2010), Vol. 21, pp. 223–232.

13. S. A. Lurie, P. A. Belov, N. P. Tuchkova, and D. B. Volkov-Bogorodsky, "Nanomechanical modeling of the nanostructures and dispersed composites," Comp. Mater. Sci. **28** (3–4), 529–539 (2003).
14. S. A. Lurie and P. A. Belov, "Cohesion field: Barenblatt's hypothesis as formal corollary of theory of continuous media with conserved dislocations," Int. J. Fract. **50** (1–2), 181–194 (2008).
15. S. A. Lurie, P. A. Belov, and N. P. Tuchkova, "The application of the multiscale models for description of the dispersed composites," J. Composites A **36**, 145–152 (2005).
16. S. A. Lurie, D. B. Volkov-Bogorodsky, V. I. Zubov, and N. P. Tuchkova, "Advanced theoretical and numerical multiscale modeling of cohesion/adhesion interactions in continuum mechanics and its applications for filled nanocomposites," Comp. Mater. Sci. **45** (3), 709–714 (2009).
17. D. B. Volkov-Bogorodsky, Yu. G. Evtushenko, V. I. Zubov, and S. A. Lurie, "Numerical–analytical estimation of the scale effects during the calculation of nanocomposite strains using the block multipole method," Vych. Mat. Mat. Fiz. **46** (7), 1318–1337 (2006).
18. S. A. Lurie and N. P. Tuchkova, "Continuum adhesion models for deformable solids and media with nanostructures," Komposity Nanostr. **2** (2), 25–43 (2009).
19. A. M. Glezer, "Structural classification of nanomaterials," Def. Razr. Mater., No. 2, 1–8 (2010).

Translated by K. Shakhlevich